Relativistic multiconfiguration method in low-energy scattering of electrons from argon atoms

P Syty and J E Sienkiewicz

Department of Theoretical and Mathematical Physics, Gdańsk University of Technology,
ul. Narutowicza 11/12, 80-952 Gdańsk, Poland

E-mail: sylas@mif.pg.gda.pl

Abstract

For the first time the differential cross sections of the elastic scattering of slow electrons from argon atoms are calculated in a relativistic multiconfiguration method. The correlation effects responsible for target polarization are treated in a relativistic configuration–interaction scheme that allows for dynamical effects. Calculations of the differential cross sections and spin polarization are discussed and compared with experimental and other theoretical data.

1. Introduction

In the past few years, the scattering of slow electrons by atoms has been extensively studied by both experimentalists and theoreticians. From the theoretical point of view, the difficulties arise from the need of precise calculations of target polarization. Present calculations are performed by using the relativistic version of the multiconfiguration and configuration–interaction (CI) approach applied to elastic electron scattering on atoms. This approach was originally developed by Sienkiewicz *et al* (1995), Sienkiewicz and Baylis (1997) and Syty (2003). The method allows for describing the polarization of different target states due to the incoming electron charge through bound relativistic configuration expansions. The target polarization is different for different kinetic energies of the incident electron, and thus dynamic effects are taken into account. The relativistic phase shifts obtained by this method are used to calculate differential cross sections and spin polarization of electron scattering by argon in its ground state at a few selected energies.

In this paper, for the first time the relativistic configuration–interaction method is applied to calculate the differential cross sections on elastic scattering of electrons from atomic target. Argon was chosen as a model example since it was extensively studied experimentally as well as theoretically. Although argon is a relatively light atom, the relativistic effects in electron scattering can be estimated (Walker 1971, Sienkiewicz and Baylis 1987).

The very first experimental measurements of differential cross sections in the scattering of slow electrons from argon atoms were performed by Ramsauer and Kollath (1929, 1932),

Hughes and McMillen (1932) and Webb (1935). Since 1970, the measurements were performed in wide range of angles by Dehmel *et al* (1976), Srivastava *et al* (1981), Furst *et al* (1989), Gibson *et al* (1996) and Panajotović *et al* (1997). Spin polarization measurements at low scattering energies were performed by Beerlage *et al* (1981).

There were many various theoretical methods used to obtain differential cross sections in scattering of electrons from argon atoms, i.e. Amusia *et al* (1982) used many-body perturbation theory, Fon *et al* (1983) and Bell *et al* (1984) used *R*-matrix method, McEachran and Stauffer (1983, 1997) and Dasgupta and Bhatia (1985) utilized polarized orbitals method. Nahar and Wadehra (1987, 1991), Sienkiewicz and Baylis (1987) and Plenkiewicz *et al* (1988) used model polarization potentials. Saha (1991) based on the multiconfiguration Hartree–Fock method. Relativistic Dirac–Fock method, in connection with model polarization potentials was used by Sienkiewicz *et al* (2001).

When compared to the other theoretical methods, the relativistic multiconfiguration method, which is used in our calculations, is more accurate in taking into account the dynamical core polarization and the electron–correlation effects, by using an *ab initio* approach. As these effects are very important in describing atomic target, we expect that our new approach should result in a better conformity with experimental data than the results obtained using other theoretical methods.

A review of the theory used in computations is presented in section 2 and the computational procedure is described in section 3. Our results are presented and compared with experiment and other available calculations in section 4. Finally, the concluding remarks are included in section 5.

2. Theory

Let us start from the relativistic scattering equation

$$H_{N+1}\Psi = \mathcal{E}\Psi, \tag{1}$$

where H_{N+1} is the $(N+1)$-electron Dirac–Coulomb Hamiltonian operator,

$$H_{N+1} = \sum_{i=1}^{N+1}\left[c\sum_{k=1}^{3}\alpha_k^i p_k^i + (\beta^i - 1)c^2 - \frac{Z}{r_i}\right] + \sum_{i=1}^{N+1}\sum_{j=i+1}^{N+1}\frac{1}{r_{ij}}, \tag{2}$$

and Ψ is the scattering state wavefunction including one electron in the continuum. In equation (2), c is the speed of light, α and β are the usual Dirac matrices, p_k is the component of an electron momentum, Z is the atomic number, r_i is the position of the ith electron, and finally, r_{ij} is the distance between ith and jth electron.

The total energy of the scattering system is

$$\mathcal{E} = E_a + E, \tag{3}$$

where E_a is the energy of the N-electron target, and E is the kinetic energy of the scattered electron.

To obtain the approximate solution of our scattering equation (1), we use the multiconfiguration Dirac–Fock method. In this method, an atomic state function (ASF) is approximated by a linear combination of configuration state functions (CSFs),

$$\Phi_a(P_a J_a M_a) = \sum_{r=1}^{n_c} b_{ar}\phi_r(N, \gamma_r J_a M_a P_a), \tag{4}$$

where P_a is the parity of the atomic state, J_a is the total angular momentum, M_a the magnetic number, and n_c is the number of CSFs. The CSFs are eigenfunctions of the parity and the

total angular momentum operators and are associated with the set of the quantum numbers $(P_a J_a M_a)$. They are built from antisymmetrized products of a common set of orthonormal Dirac orbitals

$$u_{n\kappa m}(\mathbf{r}) = \frac{1}{r}\begin{pmatrix} P_{n\kappa}(r)\chi_{\kappa m}(\mathbf{r}/r) \\ iQ_{n\kappa}(r)\chi_{-\kappa m}(\mathbf{r}/r) \end{pmatrix}, \tag{5}$$

where P_{nk} and Q_{nk} are the large and small components of the Dirac radial spinor, respectively, and the spin-angular function is given by

$$\chi_{\kappa m}(\mathbf{r}/r) = \sum_{\sigma=\pm 1/2}\left\langle jm \left| l, \frac{1}{2}, m-\sigma, \sigma \right.\right\rangle Y_l^{m-\sigma}(\mathbf{r}/r)\chi_{1/2}^{\sigma}, \tag{6}$$

where $\left\langle jm \left| l, \frac{1}{2}, m-\sigma, \sigma \right.\right\rangle$ is a Clebsch–Gordan coefficient, $Y_l^{m-\sigma}(\mathbf{r}/r)$ is a spherical harmonic, $\chi_{1/2}^{\sigma}$ is the spin eigenfunction, κ is the relativistic angular quantum number, $\kappa = \pm(j+1/2)$ for $l = j \pm 1/2$, where j is the total angular momentum, l and m are the orbital and magnetic quantum numbers, respectively.

The symbol γ_r in equation (4) denotes the occupation and the coupling of the electron subshells, and thus allows us to distinguish CSFs of the same global symmetry. The radial parts of the functions $\phi_r(N, \gamma_r J_a M_a P_a)$ as well as the mixing coefficients b_{ar} are generated in the self-consistent field (SCF) process with respect to the Dirac–Coulomb Hamiltonian.

We express the total wavefunction of the $(N+1)$-electron scattering system in the form (Burke *et al* 1971)

$$\Psi(PJM; N+1) = \mathcal{A}\sum_{a=1}^{m_a} c_a \Phi_a(P_a J_a M_a; N)u_{\kappa(a)m(a)} + \sum_{j=1}^{m_d} d_j \phi_j(PJM; N+1). \tag{7}$$

The first term on the right-hand side of equation (7) is the antisymmetrized product of the bound configuration states of the target atom and one-electron continuum spinors $u_{\kappa(a)m(a)}$.

The continuum Dirac spinor is defined as

$$u_{\kappa m}(\mathbf{r}) = \frac{1}{r}\begin{pmatrix} P_{\kappa}(r)\chi_{\kappa m}(\mathbf{r}/r) \\ iQ_{\kappa}(r)\chi_{-\kappa m}(\mathbf{r}/r) \end{pmatrix}, \tag{8}$$

where P_k and Q_k now refer to continuum orbitals.

The continuum orbitals are the solutions of the Dirac–Fock equations:

$$\left(\frac{\mathrm{d}}{\mathrm{d}r} + \frac{\kappa}{r}\right)P_{\kappa}(r) - \left(2c - \frac{E}{c} + \frac{V(r)}{cr}\right)Q_{\kappa}(r) = -\frac{X^{(P)}(r)}{r} \tag{9}$$

$$\left(\frac{\mathrm{d}}{\mathrm{d}r} - \frac{\kappa}{r}\right)Q_{\kappa}(r) + \left(-\frac{E}{c} + \frac{V(r)}{cr}\right)P_{\kappa}(r) = \frac{X^{(Q)}(r)}{r}, \tag{10}$$

where c is the speed of light, and E is the kinetic energy of the scattered electron. Direct and exchange potentials, $V(r)$ and $X(r)$, are given by Grant *et al* (1980). These equations are solved by the method of outward integration.

The first sum in equation (7) ranges over all m_a open channels Φ_a. In the case of elastic scattering, we have only one open channel, thus $m_a = 1$.

The second sum in expansion (7) accounts for correlation effects between the scattered electron and the bound target electrons. In our approach, the $(N+1)$-electron configuration state functions ϕ_j are constructed from bound-state orbitals of the target atoms, including excitations of some of the core electrons into a set of virtual orbitals.

In the case of elastic scattering, we obtain the coefficients d_j by solving the system of m_d linear equations (Saha 1991):

$$\langle \mathcal{A}\Phi u_{\kappa m}|H_{N+1} - \mathcal{E}|\phi_{j'}\rangle + \sum_{j=1}^{m_d} d_j^* \langle \phi_j|H_{N+1} - \mathcal{E}|\phi_{j'}\rangle = 0, \qquad j' = 1, \ldots, m_d. \tag{11}$$

This set of equations is derived by applying the condition that the functional $\langle \Psi|H_{N+1} - \mathcal{E}|\Psi\rangle$ must be stationary with respect to variations of the d_j coefficients.

The solution of equations (11) determines new direct and exchange potentials and, through the Dirac–Fock equations (10), an improved continuum scattering orbital. This, in turn, can be used in a new calculation of coefficients d_j. The procedure is iterated to self-consistency.

Now let us define two complex scattering amplitudes $f(\vartheta)$ (the direct amplitude) and $g(\vartheta)$ (the 'spin-flip' amplitude), according to Kessler (1985, p 35):

$$f(\vartheta) = \frac{1}{2ik} \sum_l \left\{ (l+1)\left[\exp\left(2i\delta_l^+\right) - 1\right] + l\left[\exp\left(2i\delta_l^-\right) - 1\right] \right\} P_l(\cos\vartheta), \tag{12}$$

$$g(\vartheta) = \frac{1}{2ik} \sum_l \left[\exp\left(2i\delta_l^-\right) - \exp\left(2i\delta_l^+\right)\right] P_l^1(\cos\vartheta), \tag{13}$$

where ϑ is the scattering angle, $P_l(\cos\vartheta)$ and $P_l^1(\cos\vartheta)$ are the Legendre polynomial and the Legendre associated function, respectively. The $\delta_l^\pm$ are the relativistic phase shifts, where the index '+' refers to the solution with $\kappa = -l - 1$ and '−' refers to the solution with $\kappa = l$.

Having the scattering amplitudes, we can calculate the set of observables—the differential cross section

$$\sigma(\vartheta) = |f(\vartheta)|^2 + |g(\vartheta)|^2, \tag{14}$$

and the spin polarization parameters

$$S(\vartheta) = \frac{i(f(\vartheta)g(\vartheta)^* - f(\vartheta)^* g(\vartheta))}{\sigma(\vartheta)} \tag{15}$$

$$T(\vartheta) = \frac{|f(\vartheta)|^2 - |g(\vartheta)|^2}{\sigma(\vartheta)} \tag{16}$$

$$U(\vartheta) = \frac{f(\vartheta)g(\vartheta)^* + f(\vartheta)^* g(\vartheta)}{\sigma(\vartheta)}. \tag{17}$$

These parameters are not independent, since $S + T + U = 1$. In our work, we calculate and present only the spin polarization parameter given by equation (15).

3. Computational procedure

To represent the atomic ground state (equation (4)) of the argon atom, we include 9022 relativistic configuration state functions (CSFs) with the total angular momentum 0 and even parity. These configuration states are obtained by the excitations of one or two electrons from the 3s and 3p subshells into the set of virtual orbitals 3l 4l 5d 6s 6p 6d 7s 7p 8s 8p 9s 10s. In order to obtain a full Dirac–Coulomb–Breit matrix, the contribution from the relativistic (transverse) Breit interaction between electrons has been added to the Hamiltonian matrix as a perturbation.

The atomic ground-state function and the set of configuration state functions are generated with the atomic structure program GRASP92 written by Parpia *et al* (1996).
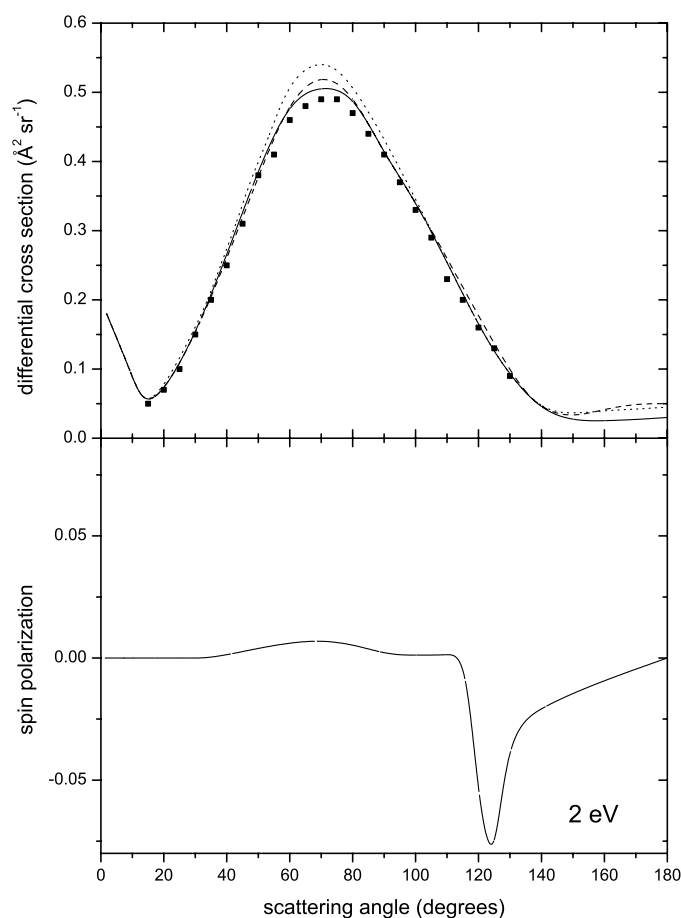
Figure 1. Differential cross section and spin polarization for elastic scattering of electrons from argon atoms, 2 eV. Solid line: present results; dashed line: theoretical results of McEachran and Stauffer (1997); dotted line: theoretical results of Sienkiewicz and Baylis (1987); full squares: experimental results of Gibson *et al* (1996).

To construct the total scattering state Ψ and to generate the continuum orbitals $u_{\kappa m}$, we use the computer code COWF developed by Fritzsche (2001). The original COWF code has been improved and modified to run on multiprocessor computers (Dziedzic *et al* 2005). The continuum orbitals are orthogonalized to the atomic orbitals by the Schmidt orthogonalization procedure.

The dominant contribution to the total dipole polarization comes from the polarization of the 3s and 3p orbitals. In our calculations, we include the dipole polarization of the target argon atom through the configuration–interaction procedure. The bound $(N + 1)$-electron configuration state functions ϕ_j (equation (7)), that account for the dipole polarization, are built of atomic orbitals 1s, 2p, ... up to 6d, obtained by the relativistic multiconfiguration self-consistent field method. We generate these configurations by the virtual excitations form the subshell 3s into the 3p 4p 5p 6p subshells and from the 3p subshells into the orbitals 3s 3d 4s 4d 5s 5d 6s 6d.
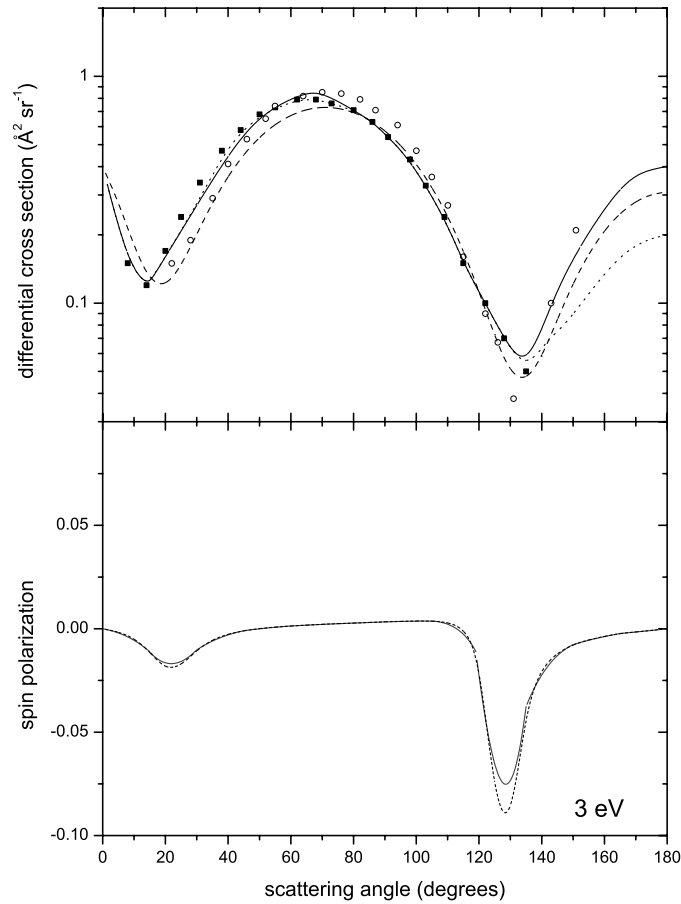
Figure 2. Differential cross section and spin polarization for elastic scattering of electrons from argon atoms, 3 eV. Solid line: present results; dashed line: theoretical results of McEachran and Stauffer (1983); dotted line: theoretical results of Saha (1996); full squares: experimental results of Gibson *et al* (1996); open circles: experimental results of Williams (1979); short-dashed line (lower graph): theoretical results of Nahar and Wadehra (1991).

The continuum orbitals and expansion coefficients d_j are determined by iteration procedure leading to self-consistency by the use of methods and computer code developed by Sienkiewicz *et al* (1995), Sienkiewicz and Baylis (1997) and Syty (2003).

Relativistic phase shifts $\delta_l^{\pm}$ are obtained by comparing the numerical solutions of continuum orbitals with the asymptotic ones at large r:

$$\frac{P_\kappa(r)}{r} \sim j_l(kr) \cos \delta_l^{\pm} - n_l(kr) \sin \delta_l^{\pm}, \tag{18}$$

where $j_l(kr)$ and $n_l(kr)$ are the Bessel and Neumman spherical functions, respectively.

We calculate the relativistic phase shifts $\delta_l^{\pm}$ for $l = 0, 1, \ldots, 10$. For higher values of the orbital momentum (up to $l = 50$), we estimate phase shifts by using the non-relativistic formula of Ali and Fraser (1977).
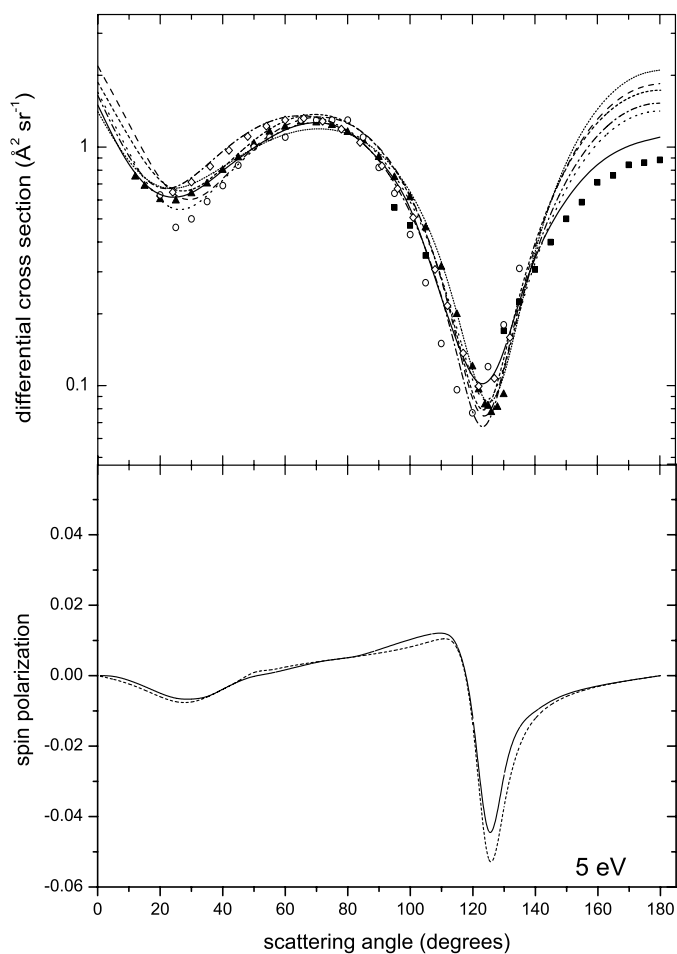
Figure 3. Differential cross section and spin polarization for elastic scattering of electrons from argon atoms, 5 eV. Solid line: present results; dashed line: theoretical results of Saha (1991); dotted line: theoretical results of Dasgupta and Bhatia (1985); dash-dotted line: theoretical results of Fon *et al* (1983); short-dashed line: theoretical results of McEachran *et al* (1997); short-dotted line: theoretical results of Gibson *et al* (1996); circles: experimental results of Srivastava *et al* (1981); triangles: experimental results of Gibson *et al* (1996); squares: experimental results of Mielewska (2003); rhombus: experimental results of Furst *et al* (1989); short-dashed line (lower graph): theoretical results of Nahar and Wadehra (1991).

4. Results

In figures 1–5, differential cross sections (14) and spin polarizations (15), for a few selected impact electron energies, are presented and compared with existing experimental and theoretical data.

Figure 1 shows our results at impact energy of 2 eV. In the case of differential cross section, we compare our results with the experimental data of Gibson *et al* (1996) and theoretical studies by Sienkiewicz and Baylis (1987) who used model polarization potential in their calculations, and McEachran and Stauffer (1997) who used polarized orbitals method. For spin polarization, at this particular energy, no comparison data are available till now. As one can see, for angles
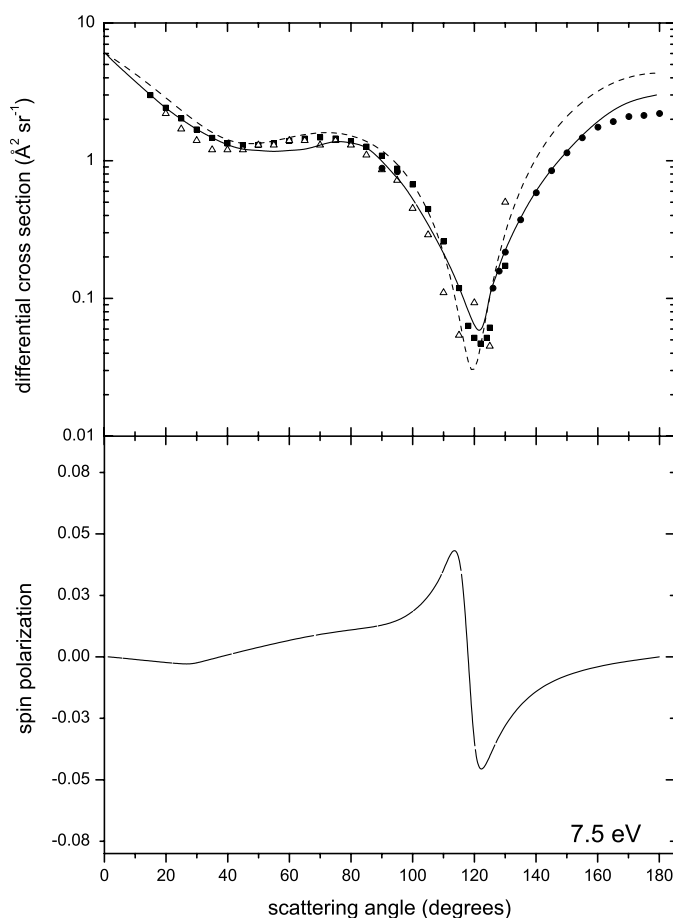
Figure 4. Differential cross section and spin polarization for elastic scattering of electrons from argon atoms, 7.5 eV. Solid line: present results; dashed line: theoretical results of Saha (1991); full squares: experimental results of Gibson *et al* (1996); full circles: experimental results of Mielewska (2003); open triangles: experimental results of Srivastava *et al* (1981).

in the ranges of 20°–60° and 80°–130°, present results (as former ones) stay in a rather good agreement with experiment. For angles 60°–80° all theoretical lines lie above the experimental points, however, our line is closest to these points. For angles above 150°, our line is somewhat below the other theoretical lines, but no experimental data are yet available to verify which line is better.

Next, we present our results at an energy of 3 eV (figure 2). Here, our results are compared with the experimental results of Gibson *et al* (1996) and Williams (1979) together with theoretical lines given by Saha (1996) who used multiconfiguration Hartree–Fock method, and McEachran and Stauffer (1983), who used polarized-orbital approximation. Spin polarization is compared to the theoretical study by Nadar and Wadehra (1991). In this case, our results are very close to results given by Saha for low and middle angles. Both lines stay in a good agreement with both experimental data sets. For big angles, present results are two times bigger than Saha's results, but thanks to this fact, they stay in a better agreement with the results of Williams. Two spin polarization lines are very similar, the only difference is the depth of the minima.
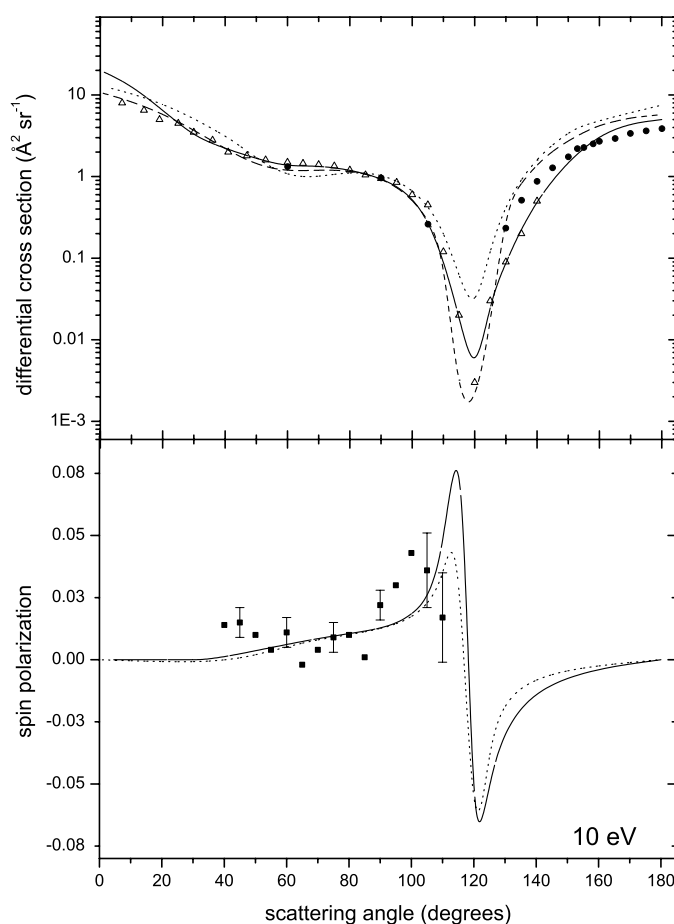
Figure 5. Differential cross section and spin polarization for elastic scattering of electrons from argon atoms, 10 eV. Solid line: present results; dotted line (upper graph): theoretical results of McEachran and Stauffer (1983); dashed line: theoretical results of Plenkiewicz *et al* (1988); full circles: experimental results of Mielewska (2003); open triangles: experimental results of Furst *et al* (1989); dotted line (lower graph): theoretical results of Nahar and Wadehra (1991); full squares: experimental results of Beerlage *et al* (1981).

The next three cases (for 5, 7.5 and 10 eV, figures 3–5) are very interesting, because experimental results are available for differential cross sections in scattering at the big angles (Mielewska 2003). We also present the experimental data of Srivastava *et al* (1981), Gibson *et al* (1996) and Furst *et al* (1989). Besides the present results obtained in relativistic multiconfiguration manner, for comparison, we also include the theoretical results of Saha (1991), Dasgupta and Bhatia (1985), Fon *et al* (1983), McEachran and Stauffer (1983, 1997), Gibson *et al* (1996) and Plenkiewicz *et al* (1988). Here, for angles up to 140°, all theoretical results stay in rather good agreement with experiment, but differences grow dramatically for bigger angles. It concerns also the present results, but let us note here that the presented results are closest to the experimental points given by Mielewska, however. It is clearly seen in figure 4 (for 7.5 eV) that our line deviates from these points only for angles above 160°. For energy of 10 eV, our line is more steep than the experimental results at the big angles, but perfectly fits to the results of Furst *et al* (1989).

For spin polarization at these energies, we observe good agreement of our results compared to the theoretical results of Nahar and Wadehra (1991). To our knowledge, for energy of 10 eV the only available experimental data are of Beerlage *et al* (1981), and are included in figure 5. The disagreement between the experimental points of Beerlage and our results can be explained by quite substantial experimental errors (see figure 5).

5. Conclusions

For the first time, relativistic multiconfiguration calculations of differential cross sections have been performed for the elastic scattering of slow electrons by atomic target. We show that our results in the case of argon stay in a good agreement with existing experimental data for all presented scattering energies. This fact was expected as the method used in calculations allows for taking into account dynamic effects in a precise *ab initio* manner through the $(N + 1)$-electron bound configurations. Our method is particularly suitable for heavier atoms, where relativistic effects play an even more important role.

It is obvious that up to now the scattering experiments are not accurate enough to provide data for very precise comparison with our theoretical data. Nevertheless, we hope that our method is a valuable step in developing theoretical methods.

The next step in improving this method should be to take into consideration inelastic channels. This would require some modifications of the method (in particular, rewriting the set of equations (11)), but would allow for much broader comparison with available experimental data.

Acknowledgments

References

Ali M A and Fraser P A 1977 *J. Phys. B: At. Mol. Phys.* **10** 3091
Amusia M Ya, Cherepkov N A, Chemysheva L V, Davidović D M and Radojević V 1982 *Phys. Rev.* A **25** 219
Beerlage M J M, Qing Z and Van der Wiel M J 1981 *J. Phys. B: At. Mol. Phys.* **14** 4627
Bell K L, Scott N S and Lennon M A 1984 *J. Phys. B: At. Mol. Phys.* **17** 4757
Burke P G, Hibbert A and Robb W D 1971 *J. Phys. B: At. Mol. Phys.* **4** 153
Dasgupta A and Bhatia A K 1985 *Phys. Rev.* A **32** 3335
Dehmel R C, Fineman M A and Miller D R 1976 *Phys. Rev.* A **13** 115
Dziedzic J, Syty P and Sienkiewicz J E 2005 in preparation
Fon W C, Berrington K A, Burke P G and Hibbert A 1983 *J. Phys. B: At. Mol. Phys.* **16** 307
Fritzsche S 2001 Private communication
Furst J E, Golden D E, Mahgerefteh M, Zhou J and Mueller D 1989 *Phys. Rev.* A **40** 5592
Gibson J C, Gulley R J, Sullivan J P, Buckman S J, Chan V and Burrow P D 1996 *J. Phys. B: At. Mol. Opt. Phys.* **29** 3177
Grant I P, McKenzie B J, Norrington P H, Mayers D F and Pyper N C 1980 *Comput. Phys. Commun.* **21** 207
Hughes A L and McMillen J H 1932 *Phys. Rev.* **39** 585
Kessler J 1985 *Polarized Electrons* 2nd edn (Berlin: Springer)
McEachran R P and Stauffer A D 1983 *J. Phys. B: At. Mol. Phys.* **16** 4023
McEachran R P and Stauffer A D 1997 *Aust. J. Phys.* **50** 511
Mielewska B 2003 *PhD Thesis* Gdańsk University of Technology
Nahar S N and Wadehra J M 1987 *Phys. Rev.* A **35** 2051
Nahar S N and Wadehra J M 1991 *Phys. Rev.* A **43** 1275

Panajotović R, Filipović D, Marinković B, Pejčev V, Kurepa M and Vušković L 1997 *J. Phys. B: At. Mol. Opt. Phys.* **30** 5877

Parpia F A, Fischer C F and Grant I P 1996 *Comput. Phys. Commun.* **94** 249

Plenkiewicz B, Plenkiewicz P and JayGerin J P 1988 *Phys. Rev.* A **38** 4460

Ramsauer C and Kollath R 1929 *Ann. Phys.* **3** 536

Ramsauer C and Kollath R 1932 *Ann. Phys. Lpz.* **12** 837

Saha H P 1991 *Phys. Rev.* A **43** 4712

Saha H P 1996 unpublished

Sienkiewicz J E and Baylis W E 1987 *J. Phys. B: At. Mol. Phys.* **20** 5145

Sienkiewicz J E and Baylis W E 1997 *Phys. Rev.* A **55** 1108

Sienkiewicz J E, Fritzsche S and Grant I P 1995 *J. Phys. B: At. Mol. Opt. Phys.* **28** L633

Sienkiewicz J E, Konopińska V, Telega S and Syty P 2001 *J. Phys. B: At. Mol. Opt. Phys.* **34** L409

Srivastava S K, Tanaka H, Chutjian A and Trajmar S 1981 *Phys. Rev.* A **23** 2156

Syty P 2003 *PhD Thesis* Gdańsk University of Technology

Walker D W 1971 *Adv. Phys.* **20** 257

Webb G M 1935 *Phys. Rev.* **47** 379

Williams J F 1979 *J. Phys. B: At. Mol. Phys.* **12** 265